

A Novel Generalized Low-Frequency Signal-Injection Method for Multistage Amplifier Linearization

Kwok-Keung M. Cheng, *Member, IEEE*, and Chi-Shuen Leung

Abstract—This paper presents for the first time the investigation of multistage amplifier linearization based on the generalized low-frequency signal-injection technique. Difference-frequency signals, generated by predistortion circuit, are fed to the biasing circuitry of a multistage amplifier for third-order intermodulation-distortion cancellation. The reason that two-stage injection shows better linearization performance than the single-stage injection case is analytically derived. Furthermore, issues on the optimum operating condition, gain error, and bandwidth limitation are also addressed. For demonstration, the measured performance of an experimental system using both the two-tone and digitally modulated test signals are shown.

Index Terms—Amplifiers, linearization, multistage.

I. INTRODUCTION

IN MANY traditional communication systems, modulation schemes such as FM and Gaussian minimum-shift keying (GMSK) are adopted, which allow the use of high-efficiency amplifiers (e.g., classes B and C) with the drawback of poor spectrum utilization. In recent years, there has been a rapid growth in the wireless market for high-speed and reliable data transmission that requires the use of advanced modulation schemes including QPSK, eight phase-shift keying (8PSK), and orthogonal frequency division multiplex (OFDM). When a digitally modulated signal is injected into the RF power amplifier, AM-to-AM and AM-to-PM distortions will be generated due to the time-varying waveform envelope. The spillover of energy into the adjacent channel causes unwanted interference and impairment of system performance. In the past years, various linearization methods [1]–[5] have been proposed that offer different degrees of performance at the expense of circuit complexity. Unfortunately, most of these methods require costly and bulky RF circuitry that is not suitable for mobile terminals. Recently, a low-frequency method [6], [7] has also been described, which offers the potential of greatly simplifying the design of linearization systems.

In this paper, a novel approach for multistage amplifier linearization based on the concept of generalized low-frequency signal injection is introduced. Third-order IMD cancellation is achieved by feeding the difference-frequency component, generated by the predistortion circuit, to the appropriate injection ports of a multistage amplifier. Unlike many conventional techniques, the proposed solution is highly stable, power

Manuscript received May 17, 2002. This work was supported by the Research Grants Council of the Hong Kong Special Administrative Region under Project Grant CUHK 4174/01E.

The authors are with the Department of Electronic Engineering, The Chinese University of Hong Kong, Shatin, Hong Kong (e-mail: kkcheng@ee.cuhk.edu.hk).

Digital Object Identifier 10.1109/TMTT.2002.807815

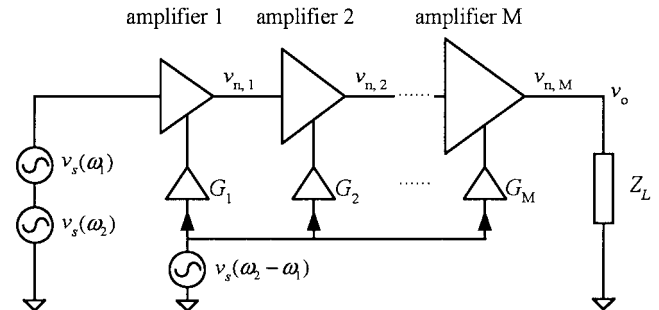


Fig. 1. System configuration.

efficient, and most important, requires no complex RF circuitry other than simple op-amps. In Section II, the reason that two-stage injection shows better linearization performance than the single-stage injection case is analytically derived. Finally, the measured performance of an experimental system using both the two-tone and digitally modulated test signals are given in Section III.

II. GENERALIZED LOW-FREQUENCY SIGNAL INJECTION

Fig. 1 shows the block diagram of the amplifying system under consideration. In practice, the transmit path of an RF front-end is usually composed of a chain of cascaded amplifiers to achieve sufficient output power and signal gain. In this figure, these amplifiers are labeled as “amplifier 1” through “amplifier M .” Furthermore, the mixing product generated by the individual nonlinear amplifier is denoted as $v_{n,m}$, where $m = 1, 2, \dots, M$. It is also assumed that an injection signal at $\omega = \omega_2 - \omega_1$ is amplified and injected into the gate input of individual RF amplifier through the corresponding biasing network.

Using the Volterra-series notation [8], and neglecting any mixing products higher than the third order, the frequency components appearing at the output of “amplifier 1” may be written as

$$\begin{aligned} v_{3,1}(2\omega_2 - \omega_1) = & \frac{3}{4} H_{3,1}(\omega_2, \omega_2, -\omega_1) \\ & \times v_s(\omega_2) v_s(\omega_2) v_s(-\omega_1) \\ & + H_{2,1}(\omega_2 - \omega_1, \omega_2) \\ & \times G_1 v_s(\omega_2 - \omega_1) v_s(\omega_2) \end{aligned} \quad (1)$$

$$\begin{aligned} v_{3,1}(2\omega_1 - \omega_2) = & \frac{3}{4} H_{3,1}(\omega_1, \omega_1, -\omega_2) \\ & \times v_s(\omega_1) v_s(\omega_1) v_s(-\omega_2) \\ & + H_{2,1}(\omega_1 - \omega_2, \omega_1) \\ & \times G_1 v_s(\omega_1 - \omega_2) v_s(\omega_1) \end{aligned} \quad (2)$$

where $H_{i,m}()$ is the i th-order nonlinear transfer function of the m th amplifier. Note that the injection signal interacts with the fundamental via the second-order nonlinear function of the amplifier to generate a new component at $\omega = 2\omega_2 - \omega_1$. Moreover, a nonlinear device is used for the generation of the difference-frequency signal from the two main tones. Without loss of generality, the relationship between the low-frequency signal and the input tones may be expressed as

$$v_s(\omega_2 - \omega_1) = K_2(\omega_2, -\omega_1) v_s(\omega_2) v_s(-\omega_1) \quad (3)$$

where $K_2()$ denotes the second-order nonlinear transfer function of the nonlinear device. Subsequently, assuming that $\omega_2 \approx \omega_1$, (1) and (2) can be rewritten as

$$\begin{aligned} v_{3,1}(2\omega_2 - \omega_1) &\approx v_{3,1}(2\omega_1 - \omega_2) \\ &= d_1 \cdot v_s(\omega_2) v_s(\omega_2) v_s(-\omega_1) \end{aligned} \quad (4)$$

where

$$d_1 = a_1 e^{j\theta_1} + G_1 b_1 e^{j\phi_1} \quad (5)$$

$$a_1 e^{j\theta_1} = \frac{3}{4} H_{3,1}(\omega_2, \omega_2, -\omega_1) \quad (6)$$

$$b_1 e^{j\phi_1} = H_{2,1}(\omega_2 - \omega_1, \omega_2) K_2(\omega_2, -\omega_1). \quad (7)$$

Similarly, the intermodulation distortion (IMD) components generated by "amplifier 2" are, therefore, given by

$$\begin{aligned} v_{3,2}(2\omega_2 - \omega_1) &= \frac{3}{4} H_{3,2}(\omega_2, \omega_2, -\omega_1) H_{1,1}(\omega_2) H_{1,1}(\omega_2) \\ &\quad \times H_{1,1}(-\omega_1) v_s(\omega_2) v_s(\omega_2) v_s(-\omega_1) \\ &\quad + H_{2,2}(\omega_2 - \omega_1, \omega_2) G_2 v_s(\omega_2 - \omega_1) \\ &\quad \times H_{1,1}(\omega_2) v_s(\omega_2) \end{aligned} \quad (8)$$

$$\begin{aligned} v_{3,2}(2\omega_1 - \omega_2) &= \frac{3}{4} H_{3,2}(\omega_1, \omega_1, -\omega_2) H_{1,1}(\omega_1) H_{1,1}(\omega_1) \\ &\quad \times H_{1,1}(-\omega_2) v_s(\omega_1) v_s(\omega_1) v_s(-\omega_2) \\ &\quad + H_{2,2}(\omega_1 - \omega_2, \omega_1) G_2 v_s(\omega_1 - \omega_2) \\ &\quad \times H_{1,1}(\omega_1) v_s(\omega_1) \end{aligned} \quad (9)$$

and the above expression may be reduced to

$$\begin{aligned} v_{3,2}(2\omega_2 - \omega_1) &\approx v_{3,2}(2\omega_1 - \omega_2) \\ &= d_2 \cdot v_s(\omega_2) v_s(\omega_2) v_s(-\omega_1) \end{aligned} \quad (10)$$

where

$$d_2 = a_2 e^{j\theta_2} + G_2 b_2 e^{j\phi_2} \quad (11)$$

$$\begin{aligned} a_2 e^{j\theta_2} &= \frac{3}{4} H_{3,2}(\omega_2, \omega_2, -\omega_1) H_{1,1}(\omega_2) \\ &\quad \times H_{1,1}(\omega_2) H_{1,1}(-\omega_1) \end{aligned} \quad (12)$$

$$b_2 e^{j\phi_2} = H_{2,2}(\omega_2 - \omega_1, \omega_2) K_2(\omega_2, -\omega_1) H_{1,1}(\omega_2). \quad (13)$$

In the general case, the IMD signal produced by "amplifier m " is simply equal to

$$\begin{aligned} v_{3,m}(2\omega_2 - \omega_1) &\approx v_{3,m}(2\omega_1 - \omega_2) \\ &= d_m \cdot v_s(\omega_2) v_s(\omega_2) v_s(-\omega_1) \end{aligned} \quad (14)$$

where

$$d_m = a_m e^{j\theta_m} + G_m b_m e^{j\phi_m}. \quad (15)$$

Consequently, the total IMD signal delivered to the load may thus be written as

$$\begin{aligned} v_o(2\omega_2 - \omega_1) &= v_{3,1}(2\omega_2 - \omega_1) \cdot T_1 + \dots \\ &\quad + v_{3,M-1}(2\omega_2 - \omega_1) \cdot T_{M-1} \\ &\quad + v_{3,M}(2\omega_2 - \omega_1) \\ &= d_M \cdot v_s(\omega_2) v_s(\omega_2) v_s(-\omega_1) \end{aligned} \quad (16)$$

where

$$T_m = \prod_{i=m+1}^M H_{1,i}(2\omega_2 - \omega_1) \quad (17)$$

$$\begin{aligned} d_M &= \{a_M e^{j\theta_M} + a_{M-1} e^{j\theta_{M-1}} T_{M-1} + \dots + a_1 e^{j\theta_1} T_1\} \\ &\quad + \{G_m b_M e^{j\phi_M} + G_{M-1} b_{M-1} e^{j\phi_{M-1}} T_{M-1} \\ &\quad + \dots + G_1 b_1 e^{j\phi_1} T_1\}. \end{aligned} \quad (18)$$

It is clear from the above expression that the output IMD signal may be viewed as the sum of two parts: the inherent IMD component (first bracket) generated by the amplifiers and the canceling signal (second bracket) produced by the injection method. Inspection of (18) also indicates that the distortion component may be eliminated with appropriate choices of the amplifier gains (G_m). It is, therefore, important to examine the different signal injection cases and related issues.

A. Amplifying System With No Signal Injection

In the absence of any injection signal ($G_m = 0$), (18) can be re-expressed as

$$\begin{aligned} |d_M| &= |a_M e^{j\theta_M} + a_{M-1} e^{j\theta_{M-1}} T_{M-1} + \dots + a_1 e^{j\theta_1} T_1| \\ &= |A e^{j\psi}|. \end{aligned} \quad (19)$$

The resultant vector $A e^{j\psi}$ represents the inherent IMD signal produced by the amplifying system and may be used as a reference level for performance evaluation.

B. Amplifying System With Single Injection Point

From the implementation point-of-view, it is simpler to use only one injection signal. Under these circumstances, (18) may be reduced to

$$|d_M| = |A e^{j\psi} + G_p b_p e^{j\phi_p} T_p| \quad (20)$$

where p ($1 \leq p \leq M$) is the number of the amplifier stage associated with the injection point. The gain coefficient for optimum IMD suppression can now be derived as

$$G_p = \frac{-A \cos(\psi - \phi_p - \angle T_p)}{b_p |T_p|}. \quad (21)$$

Hence, the achievable IMD suppression factor is simply given by

$$\left| \frac{d_M}{A} \right| = |\sin(\psi - \phi_p - \angle T_p)|. \quad (22)$$

In [6] and [7], it is assumed that the nonlinear transfer functions were real numbers (i.e., $\psi - \phi_p - \angle T_p = n\pi$) and, thus, total suppression of IMD becomes viable with single-stage injection. In practice, the value of $\psi - \phi_p - \angle T_p$ is a complex function of both device and circuit parameters [9] and, hence, only partial cancellation of IMD is possible with single-stage injection [7]. In some cases, unequal power levels of the upper and lower IMD components may be observed due to the limited cancellation capability of the conventional methods.

C. Amplifying System With Two Injection Points

In this case, an additional injection signal is fed to the input port of “amplifier q ,” and, thus, resulting IMD output can be expressed as

$$\begin{aligned} |d_M| &= |Ae^{j\psi} + G_p b_p e^{j\phi_p} T_p + G_q b_q e^{j\phi_q} T_q| \\ &= |Ae^{j\psi} + G_p b_p |T_p| e^{j\alpha} + G_q b_q |T_q| e^{j\beta}| \end{aligned} \quad (23)$$

where $\alpha = \phi_p + \angle T_p$ and $\beta = \phi_q + \angle T_q$. For complete elimination of the distortion signal, the following optimum gain conditions need to be satisfied:

$$G_p = \frac{-A}{b_p |T_p|} \cdot \frac{\sin(\psi - \beta)}{\sin(\alpha - \beta)} \quad (24)$$

$$G_q = \frac{A}{b_q |T_q|} \cdot \frac{\sin(\psi - \alpha)}{\sin(\alpha - \beta)}. \quad (25)$$

The above expressions reveal that, in the presence of the second injection signal, it is possible to eliminate the IMD signal entirely by properly adjusting the gain coefficients of the amplifiers. Equations (24) and (25) show that the gain coefficients are real with either 0° or 180° phase value and, therefore, only a constant gain amplifier is required to maintain low distortion output. According to these expressions, the gain coefficients would have unreasonably high values if α happens to be equal to β . Fortunately, this problem may easily be fixed by using a different choice of injection points.

D. Effects of Gain Error

In practice, uncertainties in gain adjustment always exist. Based on the two-stage injection method, its effect on the suppression of IMD signal may be expressed by

$$\begin{aligned} |d_M| &= |Ae^{j\psi} + (G_p + \Delta G_p) b_p |T_p| e^{j\alpha} \\ &\quad + (G_q + \Delta G_q) b_q |T_q| e^{j\beta}| \\ &= |\Delta G_p b_p |T_p| e^{j\alpha} + \Delta G_q b_q |T_q| e^{j\beta}| \end{aligned}$$

where ΔG_p and ΔG_q are the gain errors associated with the baseband amplifiers. Assuming that $\Delta G_p/G_p = \Delta G_q/G_q$, the above expression can be reduced to

$$|d_M| = \left| \frac{\Delta G_p}{G_p} \right| \cdot |G_p b_p |T_p| e^{j\alpha} + G_q b_q |T_q| e^{j\beta}|. \quad (26)$$

Consequently, we have

$$\left| \frac{d_M}{A} \right| = \left| \frac{\Delta G_p}{G_p} \right|. \quad (27)$$

Based on the above equation, the achievable IMD reduction factor is at least 30 dB provided that there are no more than 0.25-dB uncertainties in gain coefficients.

E. Bandwidth Limitation

For wide-band operation, the IMD suppression capability of the proposed method degrades progressively as the frequency spacing between the two input tones increases. Mathematically, this effect can be modeled as

$$\begin{aligned} |d_M|^2 &= |Ae^{j\psi} e^{j\Delta\psi} + G_p b_p |T_p| e^{j\alpha} e^{j\Delta\alpha} \\ &\quad + G_q b_q |T_q| e^{j\beta} e^{j\Delta\beta}|^2 \end{aligned} \quad (28)$$

where $\Delta\psi$, $\Delta\alpha$, and $\Delta\beta$ represent the phase deviation introduced by the signal paths at large tone separation. Using the assumption of small phase deviation, and by combining (24), (25), and (28), the value of $|d_M|^2$ may then be approximated by

$$\begin{aligned} |d_M|^2 &= |Ae^{j\psi} + G_p b_p |T_p| e^{j\alpha} e^{j(\Delta\alpha - \Delta\psi)} + G_q b_q |T_q| e^{j\beta} e^{j(\Delta\beta - \Delta\psi)}|^2 \\ &\approx |G_p b_p |T_p| e^{j(\alpha - \beta)} j(\Delta\alpha - \Delta\psi) + G_q b_q |T_q| j(\Delta\beta - \Delta\psi)|^2 \\ &= G_p^2 b_p^2 |T_p|^2 (\Delta\alpha - \Delta\psi)^2 + G_q^2 b_q^2 |T_q|^2 (\Delta\beta - \Delta\psi)^2 \\ &\quad + 2G_p b_p |T_p| (\Delta\alpha - \Delta\psi) G_q b_q |T_q| (\Delta\beta - \Delta\psi) \cos(\alpha - \beta). \end{aligned} \quad (29)$$

Subsequently, the IMD reduction factor can simply be written as

$$\begin{aligned} \left| \frac{d_M}{A} \right|^2 &= (\Delta\alpha - \Delta\psi)^2 \frac{\sin^2(\psi - \beta)}{\sin^2(\alpha - \beta)} \\ &\quad + (\Delta\beta - \Delta\psi)^2 \frac{\sin^2(\psi - \alpha)}{\sin^2(\alpha - \beta)} \\ &\quad + 2(\Delta\alpha - \Delta\psi)(\Delta\beta - \Delta\psi) \\ &\quad \times \frac{\sin(\psi - \alpha)\sin(\psi - \beta)\cos(\alpha - \beta)}{\sin^2(\alpha - \beta)}. \end{aligned} \quad (30)$$

The above expression shows that the operating bandwidth of this scheme is mainly determined by the phase angles ($\psi - \alpha$, $\psi - \beta$, and $\alpha - \beta$) and the group delays ($\Delta\alpha - \Delta\psi$ and $\Delta\beta - \Delta\psi$) associated with the nonlinear transfer functions. Broad-band design may, therefore, be achieved by optimizing the appropriate circuit impedance at both the fundamental and second harmonic frequencies.

III. EXPERIMENTAL RESULTS AND DISCUSSIONS

For illustrative purposes, a two-stage amplifying system operating at 2 GHz is designed (Fig. 2). The driver amplifier is built using a MESFET CFY30 with 14-dB gain and $P_{1\text{ dB}}$ of 16 dBm. The power stage is constructed using a MESFET CLY2 with 9-dB gain and $P_{1\text{ dB}}$ of 23.5 dBm. The measured gain and IMD performances of both amplifiers are shown in Fig. 3. In addition, a simple MESFET predistortion circuit, operating near pinchoff, is employed for the generation of the low-frequency injection signal. Alternatively, this signal may be extracted from the biasing network of the amplifiers. The baseband circuitry mainly

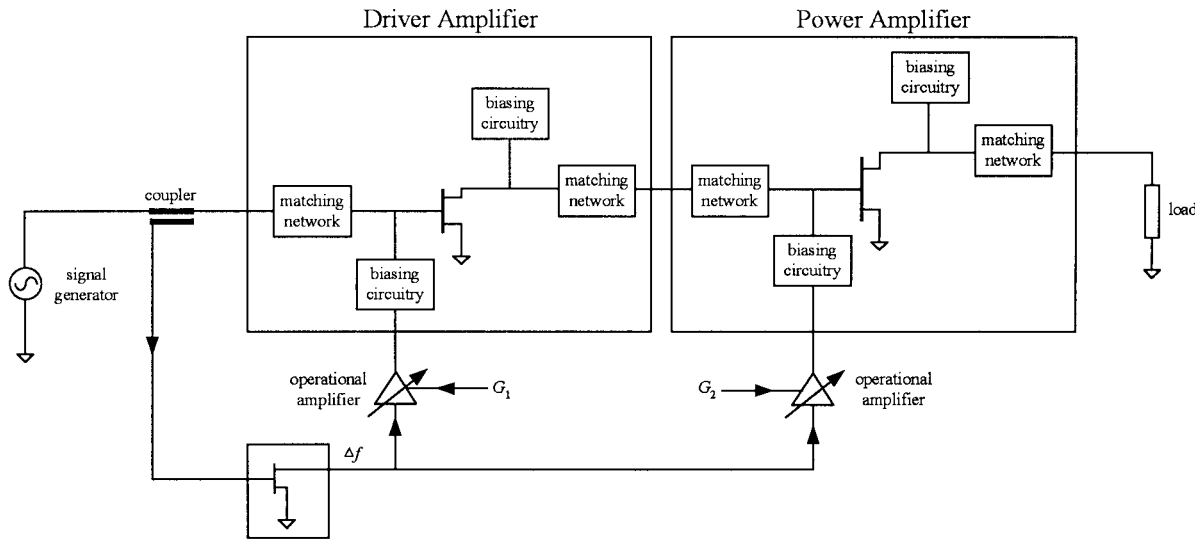
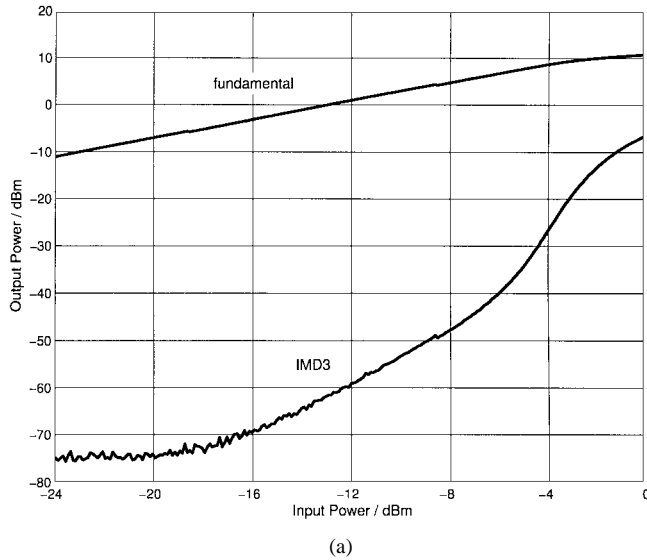
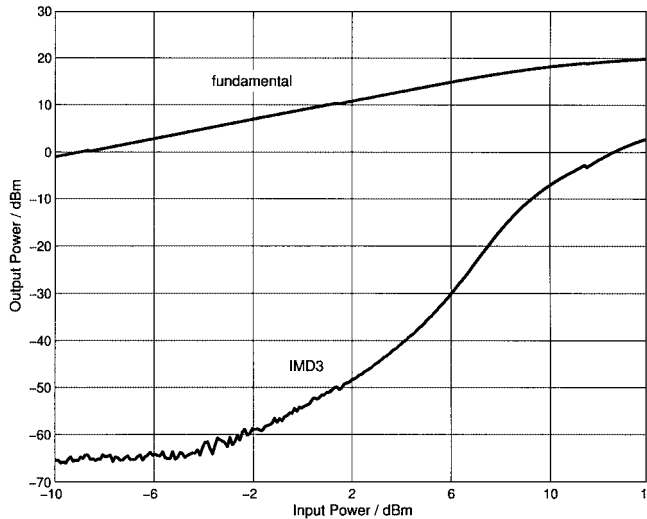


Fig. 2. Two-stage amplifying system.



(a)



(b)

Fig. 3. Measured gain and IMD performance of amplifiers: (a) Driver amplifier with 14-dB gain and $P_{1\text{dB}}$ of 16 dBm. (b) Power amplifier with 9-dB gain and $P_{1\text{dB}}$ of 23.5 dBm.

consists of low-pass filters, tunable gain operational amplifiers, and polarity inverters.

A. Determination of System Parameters and Gain Coefficients

With reference to the previous section, the IMD output and optimum gain coefficients for a two-stage amplifying system can be derived as

$$|d_2| = |Ae^{j\psi} + G_1 b_1 |T_1| e^{j\varphi_1} + G_2 b_2 |T_2| e^{j\varphi_2}| \quad (31)$$

$$G_1 = \frac{-A}{b_1 |T_1|} \cdot \frac{\sin(\psi - \varphi_2)}{\sin(\varphi_1 - \varphi_2)} \quad (32)$$

$$G_2 = \frac{A}{b_2 |T_2|} \cdot \frac{\sin(\psi - \varphi_1)}{\sin(\varphi_1 - \varphi_2)}. \quad (33)$$

It is clear from the above expressions that the gain coefficients can readily be calculated if the system parameters (A , $b_1 |T_1|$, $b_2 |T_2|$, ψ , φ_1 , and φ_2) are known. The experimental procedures for determining these parameters are given in Table I. These measurements can also be viewed as the two-tone characterization of the nonlinear transfer functions of the amplifying system. The first step ($G_1 = G_2 = 0$) involves the determination of the third-order nonlinear function of the cascaded network. The other experiments help to obtain the composite second-order transfer function associated with the two signal injection paths. The magnitudes and phases of the output vectors (d_A , d_B , and d_C) can be measured either by using the method described in [10] or by using a vector signal analyzer (see the Appendix). In these measurements, the gain value (G_B and G_C) is chosen in such a way that the third-order IMD signal is dominating and the higher order mixing products are negligibly small. The extracted values of the system parameters are tabulated in Table II for reference. Table III shows the predicted IMD performance and gain coefficients for single- and two-stage injection approaches, obtained by (21), (22), (32), and (33).

B. Performance Evaluation

For the two-tone test, signals centered at 2 GHz with frequency spacing of 100 kHz are used. For the vector signal

TABLE I
PROCEDURES FOR THE DETERMINATION OF SYSTEM PARAMETERS

G_1	G_2	d_2 (by measurement)	Formulas for parameter extraction
0	0	d_A	$Ae^{j\psi} = d_A$
G_B	0	d_B	$b_1 T_1 e^{j\varphi_1} = \frac{d_B - d_A}{G_B}$
0	G_C	d_C	$b_2 T_2 e^{j\varphi_2} = \frac{d_C - d_A}{G_C}$

TABLE II
EXTRACTED PARAMETERS OF THE EXPERIMENTAL SYSTEM

A	ψ	$b_1 T_1 $	φ_1	$b_2 T_2 $	φ_2
14.04	168.2°	3.33	293.6°	1.76	326.5°

TABLE III
PREDICTED IMD PERFORMANCE OF THE EXPERIMENTAL SYSTEM

Point of Injection	Optimum G_1	Optimum G_2	IMD Suppression Factor
Driver Amplifier	2.44	0	1.77dB
Power Amplifier	0	7.41	8.65dB
Both	-2.87	11.96	∞

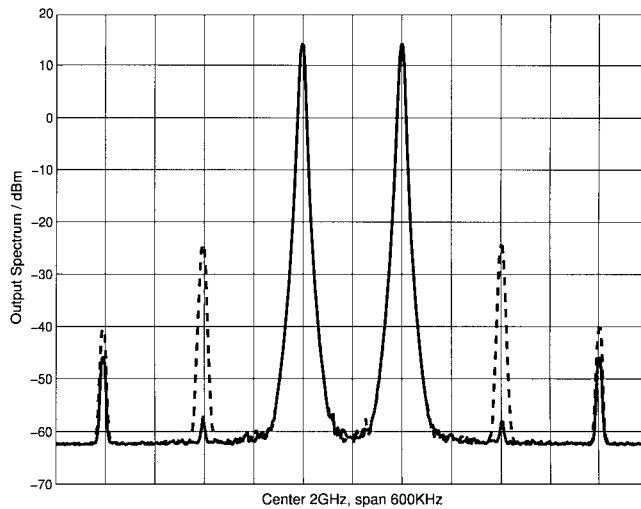
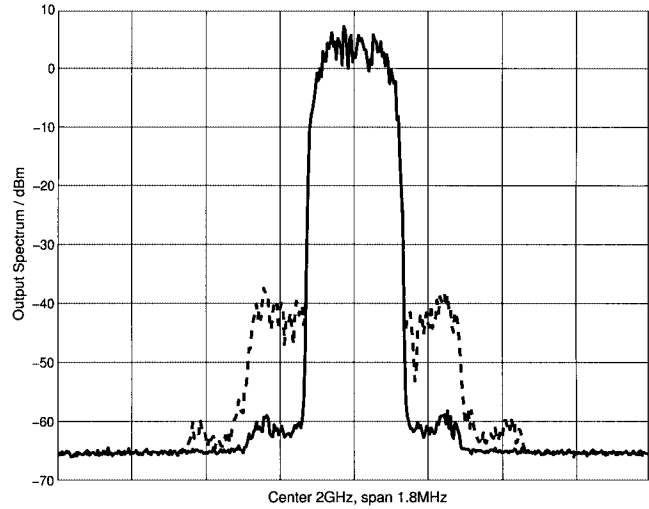


Fig. 4. Measured output spectrum test.

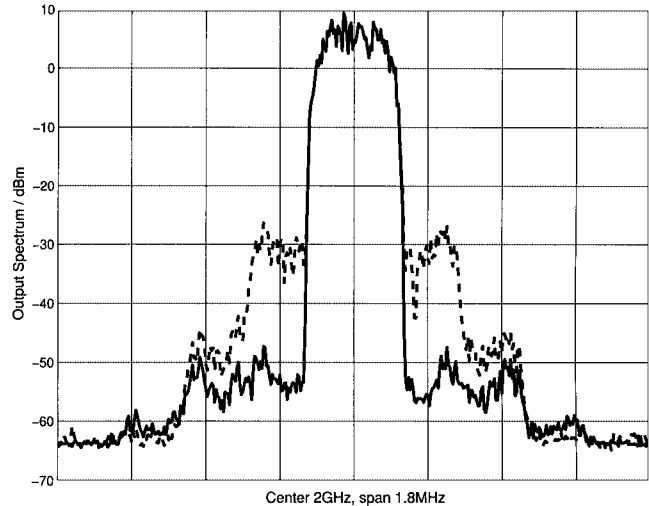
measurement, 384 kb/s $\pi/4$ differential quadrature phase-shift keying (DQPSK) personal handphone system (PHS) signal is adopted. Fig. 4 shows the measured two-tone output spectrum of the amplifying system at an output power of 14 dBm per tone. It can be seen from the diagram that the third-order IMD component is substantially suppressed (>30 dB) by feeding the injection signals to both the driver and power amplifiers. For verification purposes, the measured performance of the system with a single injection point is also given in Table IV. The limited IMD reduction factor of the amplifying system

TABLE IV
MEASURED PERFORMANCE OF THE EXPERIMENTAL SYSTEM

Point of Injection	Optimum G_1	Optimum G_2	IMD Suppression Factor
Driver Amplifier	2.27	0	1.6dB
Power Amplifier	0	6.72	8.2dB
Both	-2.99	12.60	>30 dB



(a)



(b)

Fig. 5. Output spectrums of vector signal test. (a) Average output power of 21 dBm. (b) Average output power of 23 dBm.

with single injection is approximately 1.6 dB (driver amplifier) and 8.2 dB (power amplifier), as expected. With reference to Tables III and IV, excellent agreements are observed between the measured and calculated values.

Fig. 5 shows the measured output spectrum (PHS) of the system operating at two different power levels (21 and 23 dBm). An improvement factor of approximately 20 dB in adjacent channel power ratio (ACPR) is found. Fig. 6 shows the plot of carrier-to-IMD ratio (C/I) versus output power of the amplifying system with and without linearization. The

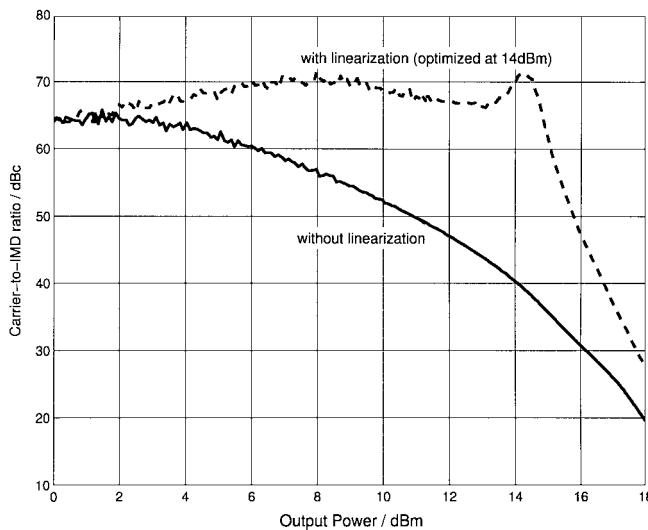


Fig. 6. Dynamic range of the proposed method.

IMD performance is optimized at an output power of 14 dBm. Without further retuning, the measurement results indicate that a C/I value of more than 65 dBc is achieved with the proposed method over a wide output power range. At a low-output power level, the result is limited only by the equipment's dynamic range. Note that the C/I performance deteriorates as the output power increases toward the 1-dB compression point. This phenomenon is believed to be due to the higher order mixing products that have not been included here. At present, the linearized system exhibits an operating bandwidth of approximately 700 kHz, with an IMD reduction factor of at least 25 dB. Bandwidth enhancement techniques are under development.

IV. CONCLUSION

The application of the generalized low-frequency signal injection method to multistage amplifier linearization has been introduced. The optimum conditions for IMD cancellation has been derived and verified. Good agreements between the predicted and measured results have been found. Substantial reduction in third-order IMD has been demonstrated for both two-tone and digitally modulated signals. Good C/I performance of the system over a wide range of output power has been observed. The proposed method requires no complex RF circuitry, which is essential to the design of a high-linearity RF amplifier for mobile applications.

APPENDIX

A vector signal analyzer provides simple and extremely fast measurements of the amplitude, frequency, and phase relationships between signal components. It uses digital signal processing (fast Fourier transform) to sample the analog input signal in the time domain and converts it to the frequency domain. Unfortunately, due to the uncorrelated phases of the input tones, the measured phase spectrum appears as random parameters. Data re-normalization is, therefore, required to recover the hidden phase information. With two-tone excitation,

the third-order IMD component at the output can be expressed as

$$\begin{aligned}
 v_o(2\omega_1 - \omega_2) &= V_o \cdot e^{j\theta_L} \cdot e^{j(2\omega_1 - \omega_2)t} \\
 &= \frac{3}{4} H_3(\omega_1, \omega_1, -\omega_2) v_s(\omega_1) \cdot v_s(\omega_1) \cdot v_s(-\omega_2) \\
 &\quad + \frac{5}{8} H_5(\omega_1, \omega_1, \omega_1, -\omega_1, -\omega_2) \cdot v_s(\omega_1) \\
 &\quad \cdot v_s(\omega_1) \cdot v_s(\omega_1) \cdot v_s(-\omega_1) v_s(-\omega_2) \\
 &\quad + \frac{5}{8} H_5(\omega_1, \omega_1, \omega_2, -\omega_2, -\omega_2) \cdot v_s(\omega_1) \\
 &\quad \cdot v_s(\omega_1) \cdot v_s(\omega_2) \cdot v_s(-\omega_2) v_s(-\omega_2) + \dots. \quad (A1)
 \end{aligned}$$

where

$$v_s(\omega_1) = A e^{j\omega_1 t + \alpha} \quad (A2)$$

$$v_s(\omega_2) = A e^{j\omega_2 t + \beta}. \quad (A3)$$

Note that $H_n(*)$ is the nonlinear transfer function of the unit under test and α and β are the random input phase variables. Hence, by combining (A1)–(A3), we obtain

$$\begin{aligned}
 v_o(2\omega_1 - \omega_2) &= v_L \cdot e^{j(2\alpha - \beta)} \cdot A^3 \cdot e^{j(2\omega_1 - \omega_2)t} \\
 &= V_L \cdot e^{j(2\alpha - \beta + \phi_L)} \cdot A^3 \cdot e^{j(2\omega_1 - \omega_2)t} \quad (A4)
 \end{aligned}$$

where

$$\begin{aligned}
 v_L &= \frac{3}{4} H_3(\omega_1, \omega_1, -\omega_2) + \frac{5}{8} H_5(\omega_1, \omega_1, \omega_1, -\omega_1, -\omega_2) \cdot A^2 \\
 &\quad + \frac{5}{8} H_5(\omega_1, \omega_1, \omega_2, -\omega_2, -\omega_2) \cdot A^2 + \dots = V_L \cdot e^{j\phi_L}. \quad (A5)
 \end{aligned}$$

The two-tone transfer characteristics of the unit (magnitude and phase of v_L) are solely dependent on the input signal strength and the nonlinear transfer functions of the unit under consideration. From (A1) and (A4), the required phase information (ϕ_L) of the lower IMD frequency component can, therefore, be derived as

$$\phi_L = \theta_L - 2\alpha + \beta \quad (A6)$$

where θ_L , α , and β are the instantaneous phase values of the main tone and IMD components captured by the vector signal analyzer. Similarly, the phase characteristics of the upper IMD component at $2\omega_2 - \omega_1$ may be evaluated by the following formula:

$$\phi_U = \theta_U - 2\beta + \alpha. \quad (A7)$$

REFERENCES

- [1] S. G. Kang, I. K. Lee, and K. S. Yoo, "Analysis and design of feedforward power amplifier," in *IEEE MTT-S Int. Microwave Symp. Dig.*, vol. 3, 1997, pp. 1519–1522.
- [2] M. R. Moazzam and C. S. Aitchison, "A low third order intermodulation amplifier with harmonic feedback circuitry," in *IEEE MTT-S Int. Microwave Symp. Dig.*, vol. 2, 1996, pp. 827–830.

- [3] N. Imai, T. Nojima, and T. Murase, "Novel linearizer using balanced circulators and its application to multilevel digital radio systems," *IEEE Trans. Microwave Theory Tech.*, vol. 37, pp. 1237–1243, Aug. 1989.
- [4] Y. Kim, Y. Yang, S. Kang, and B. Kim, "Linearization of 1.85 GHz amplifier using feedback predistortion loop," in *IEEE MTT-S Int. Microwave Symp. Dig.*, vol. 3, 1998, pp. 1675–1678.
- [5] C. W. Fan and K. K. M. Cheng, "Amplifier linearization using simultaneous harmonic and baseband injection," *IEEE Microwave Wireless Comp. Lett.*, vol. 11, pp. 404–406, Oct. 2001.
- [6] Y. Hu, J. C. Mollier, and J. Obregon, "A new method of third-order intermodulation reduction in nonlinear microwave systems," *IEEE Trans. Microwave Theory Tech.*, vol. MTT-34, pp. 245–250, Feb. 1986.
- [7] Y. Yang and B. Kim, "A new linear amplifier using low-frequency second-order intermodulation component feedforwarding," *IEEE Microwave Guided Wave Lett.*, vol. 9, pp. 419–421, Oct. 1999.
- [8] S. A. Maas, *Nonlinear Microwave Circuits*. Norwood, MA: Artech House, 1988.
- [9] C. W. Fan and K. K. M. Cheng, "Theoretical and experimental study of amplifier linearization based on harmonic and baseband signal injection technique," *IEEE Trans. Microwave Theory Tech.*, vol. 50, pp. 1801–1806, July 2002.
- [10] Y. Yang, J. Yi, J. Nam, B. Kim, and M. Park, "Measurement of two-tone transfer characteristics of high-power amplifiers," *IEEE Trans. Microwave Theory Tech.*, vol. 49, pp. 568–571, Mar. 2001.



Kwok-Keung M. Cheng (S'90–M'91) received the B.Sc. degree (with first-class honors) in electrical engineering and the Ph.D. degree from King's College, University of London, London, U.K., in 1987 and 1993, respectively.

From 1990 to 1992, he was a Research Assistant with King's College, where he was involved in the area of hybrid circuit and monolithic microwave integrated circuit (MMIC) design. From 1993 to 1995, he was a Post-Doctoral Research Associate, involved in the investigation of coplanar structures for microwave/millimeter-wave application. In 1996, he became an Assistant Professor with the Department of Electronic Engineering, The Chinese University of Hong Kong, Shatin, Hong Kong. He has authored or coauthored over 45 papers published in leading international journals and conferences, and was a contributing author of *MMIC Design* (London, U.K.: IEE Press, 1995) and *RFIC and MMIC Design and Technology* (London, U.K.: IEE Press, 2001). His current research interests are mainly concerned with the design of RF integrated circuits (RFICs)/MMICs, mixers, oscillators, power amplifiers, and linearization techniques.

Dr. Cheng was the recipient of the 1986 Siemens Prize, the 1987 Institution of Electrical Engineers Prize, and the 1988 Convocation Sesquicentennial Prize in Engineering (University of London).



Chi-Shuen Leung received the B.Eng. (with first-class honors) and M.Phil. degrees in electronic engineering from The Chinese University of Hong Kong, Shatin, Hong Kong, in 2000 and 2002, respectively.

He is currently a Research Assistant with the Department of Electronic Engineering, The Chinese University of Hong Kong. His research interests include linearization techniques, nonlinear circuit design, device modeling, and RFIC design.